Chiral Porous Metacrystals: Employing Liquid-Phase Epitaxy to Assemble Enantiopure Metal–Organic Nanoclusters into Molecular Framework Pores

Zhi-Gang Gu,[†] Hao Fu,[†] Tobias Neumann,[§] Zong-Xiong Xu,[†] Wen-Qiang Fu,[†] Wolfgang Wenzel,[§] Lei Zhang,*[,†] Jian Zhang,*[,†] and Christof Wöll*[,‡]

[†]State Key Laboratory of Structural Chemistry, Fujian Institute of Research on the Structure of Matter, Chinese Academy of Sciences, 350002 Fuzhou, P. R. China

[‡]Institute of Functional Interfaces (IFG), and [§]Institute of Nanotechnology (INT), Karlsruhe Institute of Technology (KIT), Hermann von Helmholtz Platz 1, 76344, Eggenstein Leopoldshafen, Germany

ABSTRACT: We describe the fabrication of hybrid yet well ordered porous nanoparticle (NP) arrays with full three dimensional periodicity by embedding nanometer sized metal–organic clusters (MOCs) into metal–organic frameworks (MOFs). Although conventional NP@MOF encapsulation procedures failed for these fairly large (1.66 nm diameter) NPs, we achieved maximum loading efficiency (one NP per pore) by using a modified liquid phase epitaxy (LPE) layer by layer approach to grow and load the MOF. The preformed NPs, homochiral $Ti_4(OH)_4(R/S\ BINOL)_6$ clusters (Ti MOC, BINOL = 1,1′ bi 2 naphthol), formed a regular lattice inside the pores of an achiral HKUST 1 (or $Cu_3(BTC)_2$, BTC = 1,3,5 benzenetricarboxylate) MOF thin film. Exposure to the different enantiomers of methyl lactate revealed that the NP@MOF metacrystal is quite efficient regarding enantiomer recognition and separation. The approach presented here is also suited for other MOF types and expected to provide a substantial stimulus for the fabrication of metacrystals, crystalline solids made from nanoparticles instead of atoms.

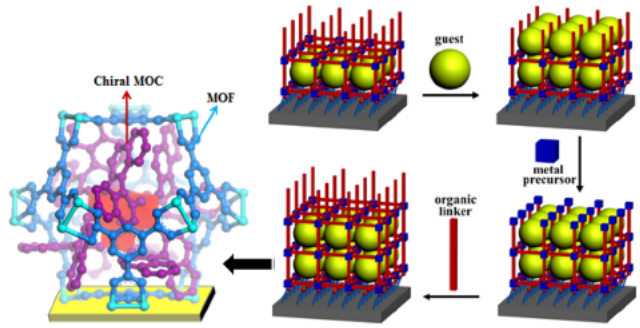

KEYWORDS: *metacrystals, metal–organic framework, nanocluster, homochirality*

Inorganic polyoxometalates (POMs) and larger metal–organic clusters (MOCs) exhibit a number of interesting catalytic properties,[1−5] Their fairly small specific surface area, however, prohibits straightforward applications in, for example, heterogeneous catalysis, homochiral synthesis, and enantiomer separation. To overcome this limitation, POMs have been successfully loaded into porous host materials.[6,7] Particularly attractive in this context are metal–organic frameworks (MOFs), which in the past decade have found numerous applications including guest storage/separation,[8,9] catalysis,[10,11] sensing,[12−14] and drug delivery,[15,16] as well as serving as a host matrix for metal ions, metallic nanoparticles (NPs), and dye molecules.[11,17−19]

In case of POMs a fairly straightforward, solvothermal route for creating NP@MOF systems can be used. Simply mixing[7,20,21] POM NPs with the reactants required for solvothermal MOF synthesis yielded loading of up to 100%, that is, one NP per MOF pore.

It would be very attractive to extend this strategy also to the larger MOCs. These NPs are particularly attractive because their fascinating structures offer many interesting properties (e.g., in asymmetric catalysis), which can be further tailored by fine tuning the organic ligands.

The chiral titanium oxo cluster $Ti_4(OH)_4(R\ BINOL)_6$ or $Ti_4(OH)_4(S\ BINOL)_6$ (BINOL = 1,1′ bi 2 naphthol) is a particular interesting case. Whereas molecular modeling (Figure S4) demonstrates that the compound fits well into the large pores of HKUST 1, unfortunately the conventional solvothermal loading procedure fails. This seems to be a general problem with MOCs, possibly to them being more fragile than POMs; a successful synthesis of MOC@MOF systems has not yet been reported.

In fact, creating metacrystals (periodic solids not composed of atoms but of nanoparticles) by assembling NPs into

Scheme 1[a]

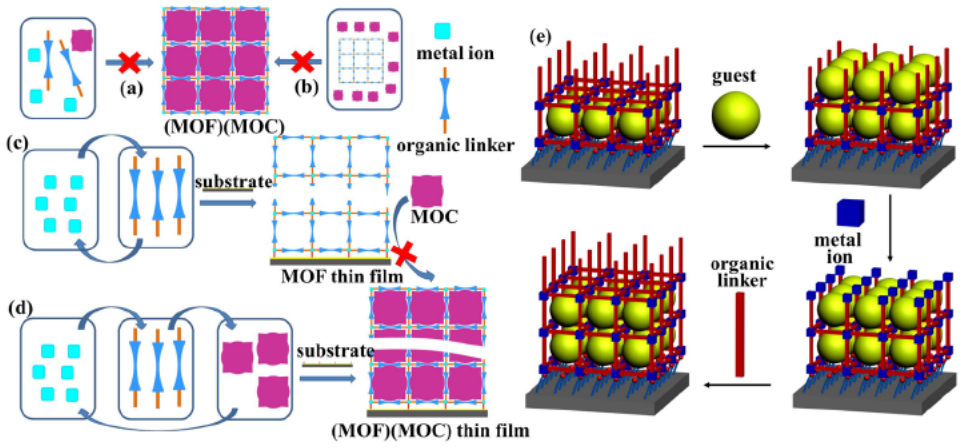

[a](a) Powder MOC loaded MOF prepared by mixing reagent of $Cu(OAC)_2$, H_3BTC, and MOC using solovothermal method (unsuccessful) (b) Powder MOC loaded MOF prepared by immersing powder MOF into MOC solution (unsuccessful). (c) Generic encapsulation of guest into MOF thin film *via* direct immersing approach (unsuccessful). (d) Layer by layer encapsulation of guest into MOF thin film *via in situ* LPE approach (successful). (e) Schematic presentation of *in situ* layer by layer growth of enantiopure Ti MOC loaded HKUST 1 thin film using the liquid phase epitaxy (LPE) approach.

three dimensional (3D) arrays is a general challenge in material science.[22−24] The most frequently used approach, crystallization of NPs exhibiting an appropriate ligand shell[25] typically yields crystalline, nonporous solids of rather poor structural order exhibiting a pronounced instability against solvents. NP arrays assembled using another method, layer by layer (lbl) deposition, has yielded higher structural order,[26] but structures with true 3D periodicity have not yet been reported. In addition, the resulting constructs do not present high stability in solvents and, more important, mostly lack porosity. The conventional metacrystal fabrication methods are thus not suited for creating porous, catalytically active MOC metacrystals for application in catalysis and enantiomer separation.

Here, we use a modified liquid phase epitaxial (LPE) process introduced recently for the fabrication of SURMOFs (surface mounted metal−organic frameworks). Because the LPE process goes through intermediate structures where half completed cages are exposed at the outer surface (see Scheme 1), it offers the chance to incorporate large, foreign species.

XRD data reveal that the LPE based loading procedure (see Scheme 1e) yields a well defined, 3D MOC NP array. The optical activity of the chiral MOC metacrystals allows the use of CD spectroscopy to demonstrate a first application: efficient enantiomer separation for methyl lactate. The method introduced here can also be applied to other MOFs and, with regard to the fabrication of metacrystals, allows definition of the periodicity of the target NP lattice, providing sufficient, tailorable porosity. This approach is also suitable for producing metacrystals from other subunits, such as nonspherical NPs.[27]

RESULTS AND DISCUSSION

The $Ti_4(OH)_4$(R/S BINOL)$_6$ clusters (R or S Ti MOC) were obtained by reactions of tetraisopropyl titanate and R/S BINOL in isopropanol/dimethylformamide (DMF) (1:1) at 60 °C for 24 h. As shown in Figure 1, in these tetranuclear Ti MOCs, each Ti(IV) ion is coordinated by six oxygen atoms from three different BINOL ligands and three μ_3 OH, forming a distorted octahedral geometry. Four Ti ions are connected together by four μ_3 OH atoms to form a cubic titanium oxo core, and this core is further surrounded by six BINOL ligands to generate the metal−organic cluster with an ∼1.66 nm diameter. Similar core structures have shown excellent performance in asymmetric catalysis,[28−30] but their enantioselective separation behaviors could not yet be studied because porous modifications of this material were not available.

HKUST 1, a standard 3D MOF with three different pore types (diameters of roughly 0.5, 1.1, and 1.35 nm[31,32]), was chosen as the host framework. Two conventional strategies were applied for the loading of the Ti MOCs into HKUST 1. First, direct synthesis was employed, using the same approach as for the previously established solvothermal POM@MOF synthesis (see above). A mixture of $Cu(OAc)_2$ (0.75 mmol), H_3BTC (0.5 mmol), and R Ti MOCs (0.25 mmol) was placed in 12 mL of ethanol at 65 °C. Even after reaction periods of 2 days, unfortunately, only a yellowish floccule was obtained. The resulting powder revealed no XRD peaks (Figure S11). In addition, CD spectra recorded for the reaction product (Figure S12) showed pronounced differences from the MOC particles dispersed in solution, demonstrating that, in the course of the solvothermal HKUST 1 synthesis, the BINOL ligands were partially detached from the central $Ti_4O_4H_4$ core.

In a second approach, powder HKUST 1 was dispersed in a fresh ethanolic solution of $Ti_4(OH)_4$(R BINOL)$_6$ (R Ti MOC, 0.1 mM, drops of DMF for promoting dissolution) for 12 h. The unchanged powder XRD and infrared (IR) (Figure S10) result showed that no guest R Ti MOC NPs were loaded in the host MOF. We explain this finding by the fact that the size of the window (1.11 nm) that separates the larger pores in HKUST 1 is much smaller than that of the present titanium oxo cluster (1.66 nm). As a result, diffusion of Ti MOCs into HKUST 1 was effectively prohibited.

After the failure of the conventional NP embedding procedures (Scheme 1a−c), we employed a recently introduced lbl synthesis method (Scheme 1d and e). This LPE approach has the potential to overcome the limitation of the NP encapsulation methods because after the step where the organic ligands (here H_3BTC) are attached to the top of the already grown MOF thin film, the walls of the top cages are not closed, and the pores can thus be loaded with objects larger than the channels separating the pores in the final framework structure. In addition, the LPE

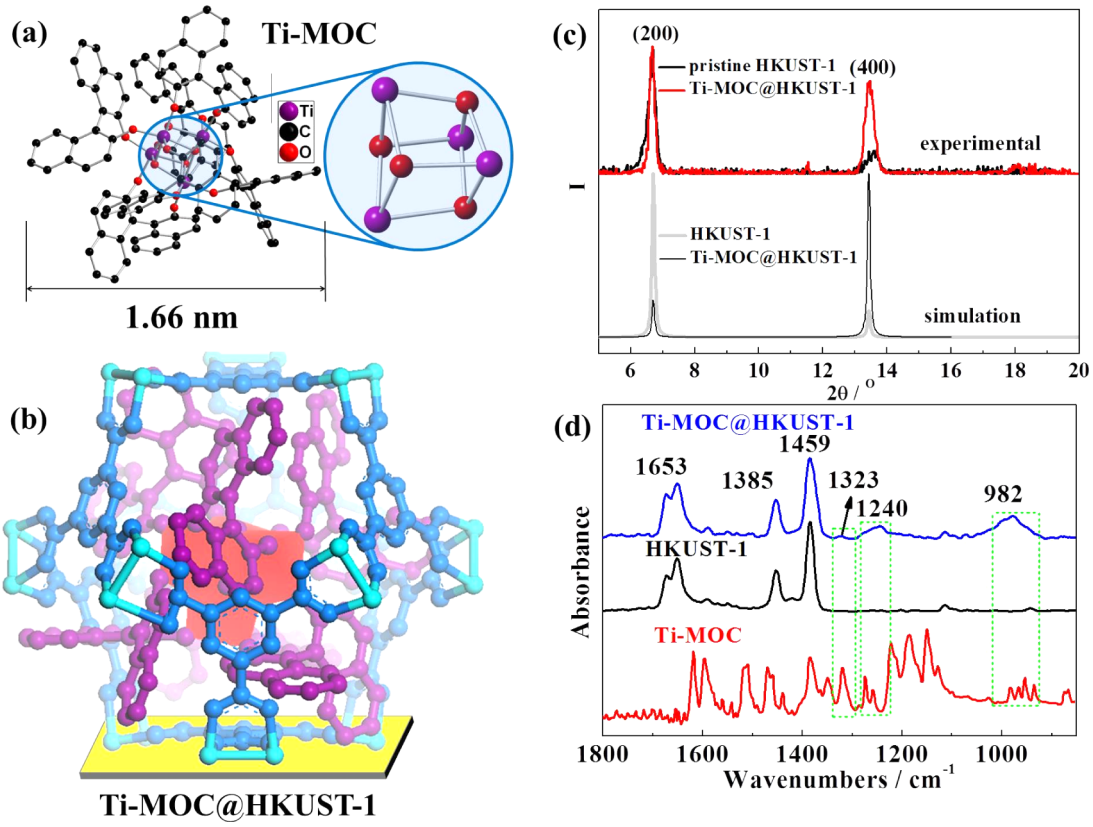

Figure 1. (a) Structure of the R Ti MOC clusters. (b) Schematic presentation of *in situ* layer by layer growth of enantiopure Ti MOC loaded HKUST 1 thin film using liquid phase epitaxy (LPE) approach. Characterization of chiral Ti MOC loaded HKUST 1 thin film *via an in situ* lbl LPE approach: (c) XRD and (d) IRRAS (infrared reflection absorption spectroscopy).

allows for much milder reaction conditions because HKUST 1 MOFs can be fabricated at room temperature; in conventional solvothermal synthesis, typically temperatures above 100 °C are employed. The LPE process used here was modified relative to one described in earlier work[33] by introducing an additional step, immersion into a solution of Ti MOC, after the H_3BTC step. We used the spray version of the LPE process[34] and applied $Cu(OAc)_2$, H_3BTC, and Ti MOC in a sequential fashion (Figure S2). Between each step, the substrate was rinsed with pure ethanol.

The LPE process was developed originally for the preparation of thin, high quality MOF coatings to be used as model systems for studying, for example, fundamental processes (diffusion, optical, and electrical properties[13,35−37]) of MOFs. An important advantage of the LPE process is that the resulting material is obtained in the form of monolithic thin films, which allow, for example, the fabrication of sensors,[13,38] high quality membranes,[39] and electrodes to be used in electrochemistry in a straightforward fashion.

After 60 LPE cycles, a thin MOF film was obtained, which in the following is referred to as (HKUST 1)(Ti MOC) SURMOF. XRD scans recorded in an out of plane geometry for a HKUST 1 SURMOF grown on a COOH terminated substrate (Figure 1c) revealed peaks at 6.8° and 13.6°, identified as the (200) and (400) reflections of HKUST 1, demonstrating the presence of a well defined, highly oriented HKUST 1 thin film, in analogy to previous work.[33] The absence of diffraction peaks for other HKUST 1 orientations demonstrated the presence of an oriented thin film, with the [100] orientation perpendicular to the substrate (Figure 1c). XRD data recorded for the NP loaded (HKUST 1)(Ti MOC) SURMOF (see Figure 1c) revealed a degree of crystallinity similar to that of the empty MOF. The infrared reflection absorption spectroscopy of Ti MOC@HKUST 1 showed that the absorbance bands at 1323, 1240, and 982 cm^{-1} are ascribed to C−O vibrations of Ti MOC (Figure 1d). Note that the relative intensities of the (400) and (200) diffraction peaks were strongly different after loading with the Ti MOC, revealing that within the host framework, a periodic array of Ti MOC NPs had formed. Based on these results, we propose a structural model in which each large pore of the HKUST 1 SURMOF contains one MOC particle (Figure 1b). Comparison of XRD simulations carried out for this model with the experimental data (see Figure 1c) reveals good agreement.

SEM images (Figure 2), TEM images, and electron mapping (Figure 3) recorded for the (HKUST 1)(Ti MOC) thin films show that the Ti MOC guests loaded in HKUST 1 have a compact and homogeneous distribution. Presumably because of a low threshold for beam damage, individual NPs could not be resolved. The TEM EDS data (Figure 3a) and the SEM EDS data of a sample cross section both gave a Cu/Ti molar ratio of 3:1. The ratio between Cu atoms and the large pores in HKUST 1 was to 12:1.[40] Considering that each Ti MOC contains four Ti atoms, we conclude that virtually every large pore in our HKUST 1 MOF thin films contains a chiral Ti MOC, in accord with the model proposed above. The IR absorbance bands at 1323, 1240, and 982 cm^{-1} are ascribed to C−O vibrations of R Ti MOC and demonstrate that the Ti MOC loaded into the MOF cages is fully intact.

To demonstrate the huge potential of these porous homo chiral metacrystals, (HKUST 1)(Ti MOC), SURMOFs were

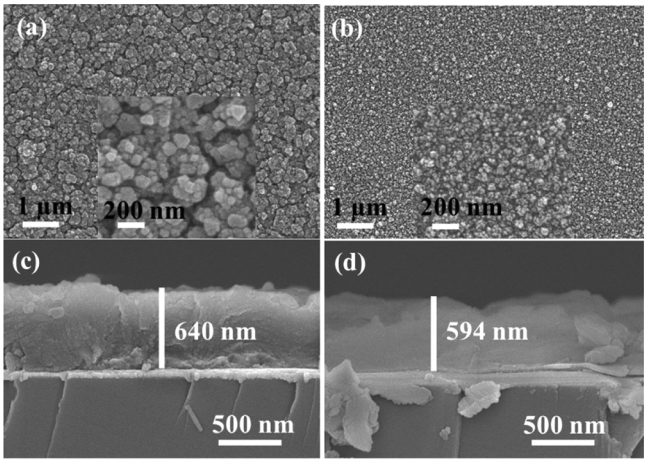

Figure 2. SEM and cross section images of (HKUST 1)(Ti MOC) thin film prepared by using LPE Ti MOC encapsulation in a lbl fashion (a,c) and pristine HKUST 1 thin film (b,d).

grown on OH functionalized quartz glass substrates, which allow recording of CD data.[41] The CD spectrum recorded for such thin films (which on this surface grow along the different, (111) orientation; Figure S3) is almost identical to that of R Ti MOC (Figure 4a) but different from spectra recorded for the free R BINOL ligands recorded in solution. This observation confirms again the successful encapsulation of intact Ti MOCs into the HKUST 1 thin film. In the following, R Ti MOC (S Ti MOC) denotes a Ti MOC with R binol (S binol) ligands. Correspond ingly, (HKUST 1)(X Ti MOC) is a HKUST 1 loaded with X Ti MOC, with X = R or X = S.

Moreover, the ESI (electron spray ionization) mass spectrum study (Figure 5a) combined with identical liquid and solid CD spectra (Figure 5b) of the chosen Ti MOCs demonstrates that the Ti MOC is stable in ethanol/DMF solution; leaching of Ti MOCs out of the NP@MOF structure was not observed. Identical results were obtained when loading with S Ti MOC (Figure 4a).

The UV−vis spectrum (Figure 6) shows the presence of a smooth homogeneous film of optical quality comparable to that of the pristine HKUST 1 SURMOF.

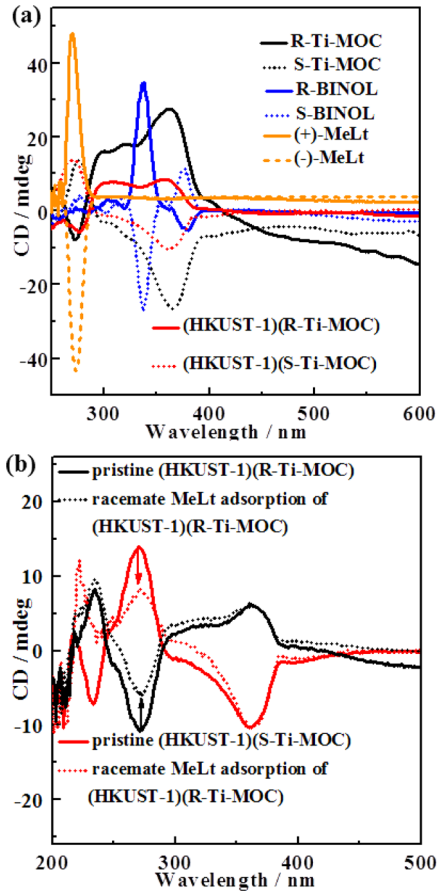

Figure 4. (a) CD spectrum of R/S BINOL, Ti_4O_4(R/S BINOL)$_6$, and Ti_4O_4(R/S BINOL)$_6$ loaded HKUST 1 prepared using the LPE lbl approach. (b) CD spectrum of pristine (HKUST 1)(R Ti MOC) and (HKUST 1)(S Ti MOC) thin films before and after adsorption of racemate methyl lactate.

To illustrate the general nature of our new lbl embedding approach, we also have demonstrated the encapsulation method for other MOF hosts, including Cu(bdc) SURMOF 2[42] and a Cu_2(D cam)$_2$dabco layer pillar type MOF[43] (bdc =1,4 benzenedicarboxylate; D cam = (1*R*,3*S*) camphorate and

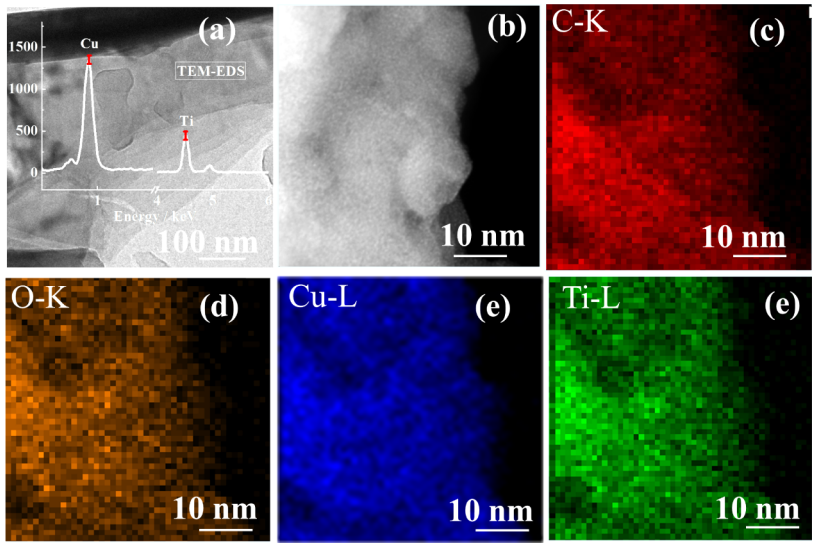

Figure 3. TEM EDS (a) and element mapping (b−e) of R Ti MOC encapsulated HKUST 1 thin film *via in situ* layer by layer LPE approach.

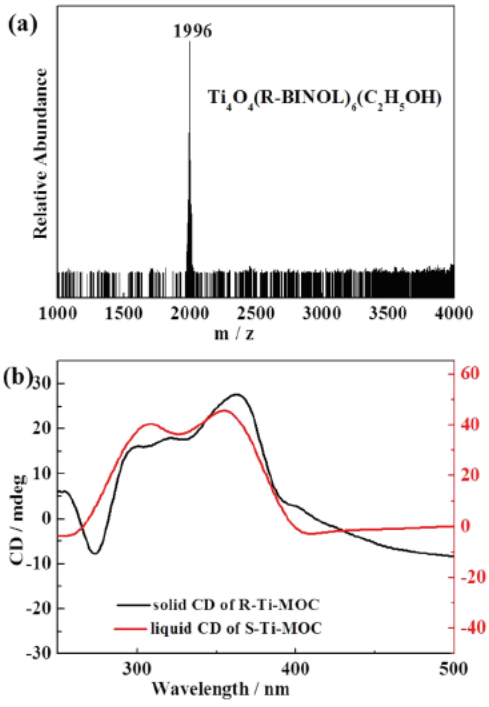

Figure 5. (a) Mass spectra of Ti_4O_4(R BINOL)$_4$ (R Ti MOC) in DMF/ethanol solution. (b) Solid and liquid CD of Ti_4O_4(R BINOL)$_4$ (R Ti MOC).

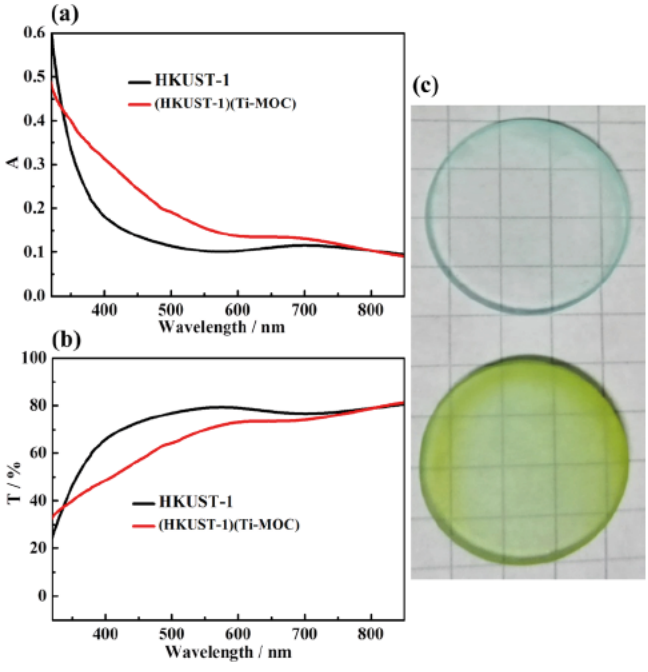

Figure 6. UV−vis absorbance (a) and transmission (b) spectra of the (HKUST 1)(Ti MOC) thin film prepared by using LPE Ti MOC encapsulation in a lbl fashion and the pristine HKUST 1 thin film. (c) Optical images of the sample SURMOF HKUST 1 (top) and (HKUST 1)(Ti MOC) thin film (bottom).

dabco =1,4 diazabicyclo[2.2.2]octane). The corresponding XRD, IR reflection absorption spectroscopy (IRRAS), and CD results (see the Supporting Information, Figures S8−S10) reveal that for these two MOFs with a structure rather different from that of HKUST 1, (MOF)(MOC) systems could be successfully prepared. This observation suggests that many (possibly all) MOF types suited for the SURMOF process also are suited for encapsulating guest species via the *in situ* LPE approach described here.

We now come to a first application of the homochiral, porous NP@MOF thin films fabricated through the *in situ* LPE process. Encapsulation of chiral Ti MOCs in the HKUST 1 MOF results in many small chiral pores in the framework, which are ideally suited for enantiomer recognition. Methyl D lactate ((+) MeLt) and methyl L lactate ((−) MeLt) were selected as model enantiomers to study the enantiomer recognition ability of the R or S Ti MOC loaded HKUST 1 thin film. The CD spectra of (+) MeLt and (−) MeLt display strong bands at ∼270 nm (Figure S5) and positive signal for (+) MeLt and negative signal for (−) MeLt), which provides a sensitive probe method for recognition. The pristine (HKUST 1)(R Ti MOC) composite film was immersed in racemic methyl lactate solution for 5 h and then cleaned thoroughly with pure ethanol. As shown in Figure 4b, the negative CD signal at ∼270 nm decreased significantly after absorption. Due to the fact that the CD signatures of the binol linkers (band at ∼335 nm) and the chiral analyte (+)/(−) MeLt (band at ∼270 nm) used in our experiments is quite different, we can directly use the intensity of this peak at 270 nm to determine the separation efficiency. Considering that, at ∼270 nm, both the (HKUST 1)(R Ti MOC) composite film and (−) MeLt have negative signal while (+) MeLt has positive signal, it can be concluded that the decrease in the negative adsorption has to be attributed to the pronounced enrichment of (+) MeLt in the film. In the same way, when (HKUST 1)(S Ti MOC) composite film was used for the enantiomer recognition measurement, positive signal at ∼270 nm also presented an obvious decrease because of the enrichment of negatively adsorbed (−) MeLt molecules (Figure 4b). Therefore, the present homochiral Ti MOC−loaded MOF film shows significant abilities for the recognition and separation of (+) MeLt and (−) MeLt enantiomers.

CONCLUSION

In conclusion, we have developed an *in situ* LPE lbl approach for the fabrication of NP metacrystals. We demonstrate the new method for nanosized homochiral titanium oxo clusters loaded into several different molecular frameworks. The complete and homogeneous distribution of chiral, R , or S Ti MOC clusters in an HKUST 1 are confirmed by CD, IR, UV−vis, SEM, and TEM EDS studies. We also demonstrated that the encapsulation of the homochiral Ti MOCs endows the highly ordered and homogeneous (MOF) (MOCs) film with significant enantiomer recognition ability, which can be used to recognize and separate (+) MeLt and (−) MeLt. Our work provides a new and versatile approach for the loading of a broad range of discrete nanometer sized guest NPs into MOFs, thus opening the way to the fabrication of highly heterogeneous, multifunctional, and porous materials with numerous applications, in particular in catalysis, enantiomer separation, and sensing.

EXPERIMENTAL SECTION

Materials and Instrumentation. All reagents and solvents employed were commercially available and used as received without further purification. The samples grown on functionalized Au substrate were characterized with IRRAS. IRRAS data were recorded using a Bruker Vertex 70 FTIR spectrometer with 2 cm^{-1} resolution at an angle of incidence of 80° relative to the surface normal. Powder XRD (PXRD) analysis was performed on a MiniFlex2 X ray diffractometer using Cu Kα radiation (λ = 0.1542 nm) in the 2θ range of 4−20° with a scanning

rate of 0.5° min^{-1}. CD experiments were recorded with a Biologic MOS 450 CD Spectrometer at room temperature. CD spectra recorded for the pure quartz glass plate (which was also used as the substrate for SURMOF thin film preparation) were used as a reference. CD spectra were recorded from 600 to 200 nm in 1 nm steps using a scan speed of 20 nm min^{-1}. TEM images and EDS recorded for Ti MOC−loaded HKUST 1 thin films were recorded using a JEM 2010F instrument. The mass of the titanium oxo cluster was determined by mass spectroscopy (DECAX 30000). SEM images for the morphology of thin films were measured using the JSM6700.

Synthesis of $Ti_4(OH)_4$(R/S-BINOL)$_6$ (R-Ti-MOC and S−Ti-MOC). A mixture of R or S BINOL (286 mg, 1 mmol, BINOL = 1,1′ bi 2 naphthol; tetraisopropyl titanate 0.6 mL, 2 mmol; isopropanol 1 mL; DMF 1 mL) was sealed in a 10 mL glass bottle, heated at 60 °C for 24 h, and cooled to room temperature. The red bulk crystals R Ti MOC and S Ti MOC were collected for characterization.

Preparation of Functionalized Substrates. The OH function alized self assembled monolayers (SAMs) on Au were prepared by immersing Au substrates into 1 mM/L ethanolic solutions of 11 mercapto 1 undecanol (MUD) for 24 h and then rinsed with the pure ethanol and dried under nitrogen flux for the next preparation.

The OH terminated quartz glass substrates were treated with a mixture of concentrated sulfuric acid and hydrogen peroxide (30%) with a volume ratio 3:1 at 80 °C for 30 min and then cleaned with deionized water and dried under nitrogen flux for the next preparation.

Synthesis of SURMOF HKUST-1 Thin Film. The HKUST 1 thin film was fabricated using the following diluted ethanolic solutions: copper acetate (1 mM) and BTC (1,3,5 benzenetricarboxylic acid) (0.4 mM). The spray method adopted in this work has been described previously.[34] The spray times were 15 s for the copper acetate solution and 25 s for the BTC solution. Each step was followed by a spray step with pure ethanol to remove residual reactants. A total of 60 growth cycles were used for HKUST 1 grown on functionalized (deposition of mercaptohexadecanoic acid (MHDA) based SAM) Au substrates. (SAMs = self assembled monolayers) and on OH terminated quartz glass substrates.

Direct Immersion of HKUST-1 SURMOFs into Ti-MOC Suspension. HKUST 1 thin films on the gold or quartz glass substrates were put into a flask and then evacuated to 0.2 kPa at room temperature for 30 min. Subsequently, the sample was immersed in a freshly prepared solution of Ti_4O_4(R BINOL)$_4$ in ethanol (0.1 mM, drops of DMF for dissolving) kept at 65 °C. After an immersion time of 12 h, the sample was removed from the solution, rinsed with pure ethanol, and finally dried in a flux of nitrogen gas for further investigation.

***In Situ* LPE lbl Encapsulation of Ti-MOC into HKUST-1 Thin Film.** For in situ encapsulation, the LPE spray method mas modified by adding an additional step, the spraying of a MOC suspension. The (Ti MOC)@(HKUST 1) thin films were fabricated using the following diluted ethanolic solutions: copper acetate (1 mM) and BTC (0.4 mM) and R or S Ti MOC (0.1 mM). The spray times were 15, 25, and 10 s for Cu(OAc)$_2$, BTC, and Ti MOC solution, respectively. There was a waiting time of 30 s between steps, and each step was followed by a 3 s spray step with pure ethanol to remove residual reactants. A total of 60 growth cycles was used for *in situ* LPE lbl encapsulation of Ti MOC into HKUST 1 thin film in this work.

Synthesis of Powder HKUST-1 MOF. Powder HKUST 1 MOF was synthesized by mixing 0.15 g (0.75 mmol) of copper(II) acetate and 0.105 g (0.5 mmol) of btc (btc =1,3,5 benzenetricarboxylic acid) in 6 mL of pure ethanol in a sealed glass bottle. The reagents were mixed and dissolved in an ultrasonic bath for 30 min, followed by heating at 65 °C for 2 days and cooling to room temperature. The resulting powder was washed with pure ethanol and dried in nitrogen. By comparing with the simulated XRD of HKUST 1, the recorded XRD showed that powder HKUST 1 was synthesized (Figure S9a).

Enantiomer Recognition of (HKUST-1)(Ti-MOC) Thin Film. The enantiomer recognition of the sample was investigated using CD spectroscopy. The pristine (HKUST 1)(R Ti MOC) (or (HKUST 1) (S Ti MOC)) film was activated under 0.2 kPa at 60 °C for 2 h and then immersed in racemic methyl lactate solution for 5 h. The sample was cleaned thoroughly with pure ethanol for the CD measurement.

More experimental and characterization details, additional figures and images, XRD patterns, IR, mass spectrometry, and CD spectra are provided in the Supporting Information.

ASSOCIATED CONTENT

Supporting Information

The Supporting Information is available free of charge on the ACS Publications website at DOI: 10.1021/acsnano.5b06230.

Additional experimental and characterization details, additional figures and images, XRD patterns, IR, mass spectrometry, and CD spectra (PDF)

AUTHOR INFORMATION

Corresponding Authors

*E mail: zhj@fjirsm.ac.cn (J.Z.).
*E mail: LZhang@fjirsm.ac.cn (L.Z.).
*E mail: christof.woell@kit.edu (C.W.).

Notes

The authors declare no competing financial interest.

ACKNOWLEDGMENTS

This work was supported by the 973 program (2012CB821705) and NSFC (21425102, 21501176 and 21221001).

REFERENCES

(1) Hou, Y. Q.; Hill, C. L. Hydrolytically Stable Organic Triester Capped Polyoxometalates with Catalytic Oxygenation Activity of Formula [Rc(Ch2o)3v3p2w15o59]6 (R = Ch3, No2, Ch2oh). *J. Am. Chem. Soc.* **1993**, *115*, 11823−11830.

(2) Sartorel, A.; Carraro, M.; Bagno, A.; Scorrano, G.; Bonchio, M. Asymmetric Tetraprotonation of Gamma [(SiO4)W10O32](8) Trig gers A Catalytic Epoxidation Reaction: Perspectives in The Assignment of The Active Catalyst. *Angew. Chem., Int. Ed.* **2007**, *46*, 3255−3258.

(3) Lee, C. F.; Leigh, D. A.; Pritchard, R. G.; Schultz, D.; Teat, S. J.; Timco, G. A.; Winpenny, R. E. P. Hybrid Organic Inorganic Rotaxanes and Molecular Shuttles. *Nature* **2009**, *458*, 314−318.

(4) Kim, W. B.; Voitl, T.; Rodriguez Rivera, G. J.; Dumesic, J. A. Powering Fuel Cells with CO *via* Aqueous Polyoxometalates and Gold Catalysts. *Science* **2004**, *305*, 1280−1283.

(5) Miras, H. N.; Yan, J.; Long, D. L.; Cronin, L. Engineering Polyoxometalates with Emergent Properties. *Chem. Soc. Rev.* **2012**, *41*, 7403−7430.

(6) Maksimchuk, N. V.; Timofeeva, M. N.; Melgunov, M. S.; Shmakov, A. N.; Chesalov, Y. A.; Dybtsev, D. N.; Fedin, V. P.; Kholdeeva, O. A. Heterogeneous Selective Oxidation Catalysts Based on Coordination Polymer MIL 101 and Transition Metal Substituted Polyoxometalates. *J. Catal.* **2008**, *257*, 315−323.

(7) Sun, C. Y.; Liu, S. X.; Liang, D. D.; Shao, K. Z.; Ren, Y. H.; Su, Z. M. Highly Stable Crystalline Catalysts Based on a Microporous Metal Organic Framework and Polyoxometalates. *J. Am. Chem. Soc.* **2009**, *131*, 1883−1888.

(8) Sumida, K.; Rogow, D. L.; Mason, J. A.; McDonald, T. M.; Bloch, E. D.; Herm, Z. R.; Bae, T. H.; Long, J. R. Carbon Dioxide Capture in Metal Organic Frameworks. *Chem. Rev.* **2012**, *112*, 724−781.

(9) Furukawa, H.; Cordova, K. E.; O'Keeffe, M.; Yaghi, O. M. The Chemistry and Applications of Metal Organic Frameworks. *Science* **2013**, *341*, 974−986.

(10) Dhakshinamoorthy, A.; Asiri, A. M.; Garcia, H. Metal Organic Frameworks Catalyzed C C and C heteroatom Coupling Reactions. *Chem. Soc. Rev.* **2015**, *44*, 1922−1947.

(11) Shieh, F. K.; Wang, S. C.; Yen, C. I.; Wu, C. C.; Dutta, S.; Chou, L. Y.; Morabito, J. V.; Hu, P.; Hsu, M. H.; Wu, K. C. W.; Tsung, C. K. Imparting Functionality to Biocatalysts *via* Embedding Enzymes into Nanoporous Materials by a de Novo Approach: Size Selective Sheltering of Catalase in Metal Organic Framework Microcrystals. *J. Am. Chem. Soc.* **2015**, *137*, 4276−4279.

(12) Shekhah, O.; Liu, J.; Fischer, R. A.; Wöll, C. MOF Thin Films: Existing and Future Applications. *Chem. Soc. Rev.* **2011**, *40*, 1081−1106.
(13) Talin, A. A.; Centrone, A.; Ford, A. C.; Foster, M. E.; Stavila, V.; Haney, P.; Kinney, R. A.; Szalai, V.; El Gabaly, F.; Yoon, H. P.; Leonard, F.; Allendorf, M. D. Tunable Electrical Conductivity in Metal Organic Framework Thin Film Devices. *Science* **2014**, *343*, 66−69.
(14) Ranft, A.; Niekiel, F.; Pavlichenko, I.; Stock, N.; Lotsch, B. V. Tandem MOF Based Photonic Crystals for Enhanced Analyte Specific Optical Detection. *Chem. Mater.* **2015**, *27*, 1961−1970.
(15) Wu, Y. N.; Zhou, M. M.; Li, S.; Li, Z. H.; Li, J.; Wu, A. Z.; Li, G. T.; Li, F. T.; Guan, X. H. Magnetic Metal Organic Frameworks: gamma Fe2O3@MOFs *via* Confined *In Situ* Pyrolysis Method for Drug Delivery. *Small* **2014**, *10*, 2927−2936.
(16) Bradshaw, D.; Garai, A.; Huo, J. Metal Organic Framework Growth At Functional Interfaces: Thin Films and Composites for Diverse Applications. *Chem. Soc. Rev.* **2012**, *41*, 2344−2381.
(17) Lu, G.; Li, S. Z.; Guo, Z.; Farha, O. K.; Hauser, B. G.; Qi, X. Y.; Wang, Y.; Wang, X.; Han, S. Y.; Liu, X. G.; et al. Imparting Functionality to A Metal Organic Framework Material by Controlled Nanoparticle Encapsulation. *Nat. Chem.* **2012**, *4*, 310−316.
(18) Della Rocca, J.; Liu, D. M.; Lin, W. B. Nanoscale Metal Organic Frameworks for Biomedical Imaging and Drug Delivery. *Acc. Chem. Res.* **2011**, *44*, 957−968.
(19) Wang, H.; Xu, J.; Zhang, D. S.; Chen, Q.; Wen, R. M.; Chang, Z.; Bu, X. H. Crystalline Capsules: Metal Organic Frameworks Locked by Size Matching Ligand Bolts. *Angew. Chem., Int. Ed.* **2015**, *54*, 5966−5970.
(20) Song, J.; Luo, Z.; Britt, D. K.; Furukawa, H.; Yaghi, O. M.; Hardcastle, K. I.; Hill, C. L. A Multiunit Catalyst with Synergistic Stability and Reactivity: A Polyoxometalate Metal Organic Framework for Aerobic Decontamination. *J. Am. Chem. Soc.* **2011**, *133*, 16839−16846.
(21) Ma, F. J.; Liu, S. X.; Sun, C. Y.; Liang, D. D.; Ren, G. J.; Wei, F.; Chen, Y. G.; Su, Z. M. A Sodalite Type Porous Metal Organic Framework with Polyoxometalate Templates: Adsorption and Decom position of Dimethyl Methylphosphonate. *J. Am. Chem. Soc.* **2011**, *133*, 4178−4181.
(22) Collier, C. P.; Saykally, R. J.; Shiang, J. J.; Henrichs, S. E.; Heath, J. R. Reversible Tuning of Silver Quantum Dot Monolayers Through The Metal Insulator Transition. *Science* **1997**, *277*, 1978−1981.
(23) Cheng, W. L.; Park, N. Y.; Walter, M. T.; Hartman, M. R.; Luo, D. Nanopatterning Self Assembled Nanoparticle Superlattices by Mould ing Microdroplets. *Nat. Nanotechnol.* **2008**, *3*, 682−690.
(24) Chen, W. J.; Jiang, S. J.; Chen, X. D.; Zhu, B. C.; Zhou, L.; Dong, J. W.; Chan, C. T. Experimental Realization of Photonic Topological Insulator in A Uniaxial Metacrystal Waveguide. *Nat. Commun.* **2014**, *5*, 5782.
(25) Miszta, K.; de Graaf, J.; Bertoni, G.; Dorfs, D.; Brescia, R.; Marras, S.; Ceseracciu, L.; Cingolani, R.; van Roij, R.; Dijkstra, M.; et al. Hierarchical Self Assembly of Suspended Branched Colloidal Nano crystals into Superlattice Structures. *Nat. Mater.* **2011**, *10*, 872−876.
(26) Srivastava, S.; Kotov, N. A. Composite Layer by Layer (LBL) Assembly with Inorganic Nanoparticles and Nanowires. *Acc. Chem. Res.* **2008**, *41*, 1831−1841.
(27) Hirai, K.; Yeom, B.; Chang, S. H.; Chi, H.; Mansfield, J. F.; Lee, B.; Lee, S.; Uher, C.; Kotov, N. A. Coordination Assembly of Discoid Nanoparticles. *Angew. Chem., Int. Ed.* **2015**, *54*, 8966−8970.
(28) Saruhashi, K.; Kobayashi, S. Remarkably Stable Chiral Zirconium Complexes for Asymmetric Mannich Type Reactions. *J. Am. Chem. Soc.* **2006**, *128*, 11232−11235.
(29) Balsells, J.; Davis, T. J.; Carroll, P.; Walsh, P. J. Insight into The Mechanism of The Asymmetric Addition of Alkyl Groups to Aldehydes Catalyzed by Titanium BINOLate Species. *J. Am. Chem. Soc.* **2002**, *124*, 10336−10348.
(30) Mahrwald, R.; Schetter, B. Unusual Highly Regioselective Direct Aldol Additions with A Moisture Resistant and Highly Efficient Titanium Catalyst. *Org. Lett.* **2006**, *8*, 281−284.
(31) Mason, J. A.; Veenstra, M.; Long, J. R. Evaluating Metal Organic Frameworks for Natural Gas Storage. *Chem. Sci.* **2014**, *5*, 32−51.
(32) Chui, S. S. Y.; Lo, S. M. F.; Charmant, J. P. H.; Orpen, A. G.; Williams, I. D. A Chemically Functionalizable Nanoporous Material [Cu 3(TMA)(2)(H2O)(3)](n). *Science* **1999**, *283*, 1148−1150.
(33) Shekhah, O.; Wang, H.; Kowarik, S.; Schreiber, F.; Paulus, M.; Tolan, M.; Sternemann, C.; Evers, F.; Zacher, D.; Fischer, R. A.; et al. Step by Step Route for The Synthesis of Metal Organic Frameworks. *J. Am. Chem. Soc.* **2007**, *129*, 15118−15119.
(34) Arslan, H. K.; Shekhah, O.; Wohlgemuth, J.; Franzreb, M.; Fischer, R. A.; Wöll, C. High Throughput Fabrication of Uniform and Homogenous MOF Coatings. *Adv. Funct. Mater.* **2011**, *21*, 4228−4231.
(35) Heinke, L.; Gu, Z. G.; Wöll, C. The Surface Barrier Phenomenon At The Loading of Metal Organic Frameworks. *Nat. Commun.* **2014**, *5*, 4562.
(36) Dragasser, A.; Shekhah, O.; Zybaylo, O.; Shen, C.; Buck, M.; Wöll, C.; Schlettwein, D. Redox Mediation Enabled by Immobilised Centres in The Pores of A Metal Organic Framework Grown by Liquid Phase Epitaxy. *Chem. Commun.* **2012**, *48*, 663−665.
(37) Liu, J. X.; Wachter, T.; Irmler, A.; Weidler, P. G.; Gliemann, H.; Pauly, F.; Mugnaini, V.; Zharnikov, M.; Wöll, C. Electric Transport Properties of Surface Anchored Metal Organic Frameworks and The Effect of Ferrocene Loading. *ACS Appl. Mater. Interfaces* **2015**, *7*, 9824−9830.
(38) So, M. C.; Jin, S.; Son, H. J.; Wiederrecht, G. P.; Farha, O. K.; Hupp, J. T. Layer by Layer Fabrication of Oriented Porous Thin Films Based on Porphyrin Containing Metal Organic Frameworks. *J. Am. Chem. Soc.* **2013**, *135*, 15698−15701.
(39) Shekhah, O.; Swaidan, R.; Belmabkhout, Y.; du Plessis, M.; Jacobs, T.; Barbour, L. J.; Pinnau, I.; Eddaoudi, M. The Liquid Phase Epitaxy Approach for The Successful Construction of Ultra Thin and Defect Free ZIF 8 Membranes: Pure and Mixed Gas Transport Study. *Chem. Commun.* **2014**, *50*, 2089−2092.
(40) Guo, W.; Liu, J. X.; Weidler, P. G.; Liu, J. X.; Neumann, T.; Danilov, D.; Wenzel, W.; Feldmann, C.; Wöll, C. Loading of Ionic Compounds into Metal Organic Frameworks: A Joint Theoretical and Experimental Study for The Case of La3+. *Phys. Chem. Chem. Phys.* **2014**, *16*, 17918−17923.
(41) Gu, Z. G.; Burck, J.; Bihlmeier, A.; Liu, J. X.; Shekhah, O.; Weidler, P. G.; Azucena, C.; Wang, Z. B.; Heissler, S.; Gliemann, H.; et al. Oriented Circular Dichroism Analysis of Chiral Surface Anchored Metal Organic Frameworks Grown by Liquid Phase Epitaxy and upon Loading with Chiral Guest Compounds. *Chem. Eur. J.* **2014**, *20*, 9879−9882.
(42) Liu, J. X.; Lukose, B.; Shekhah, O.; Arslan, H. K.; Weidler, P.; Gliemann, H.; Brase, S.; Grosjean, S.; Godt, A.; Feng, X. L. A Novel Series of Isoreticular Metal Organic Frameworks: Realizing Metastable Structures by Liquid Phase Epitaxy. *Sci. Rep.* **2012**, *2*, 921.
(43) Liu, B.; Shekhah, O.; Arslan, H. K.; Liu, J. X.; Wöll, C.; Fischer, R. A. Enantiopure Metal Organic Framework Thin Films: Oriented SURMOF Growth and Enantioselective Adsorption. *Angew. Chem., Int. Ed.* **2012**, *51*, 807−810.